Fractography of Corrosion Fatigue Cracks in RPV Steels in Pressurised Water Reactor Environments

A. N. GREENWOOD and D. R. TICE
UKAEA Northern Research Laboratories, Springfields, Salwick, Preston PR4 0RR, UK

ABSTRACT

Fractographic examination has been performed on a number of corrosion fatigue specimens, which had been exposed to a 290 C aqueous environment simulating the primary coolant of an operating Pressurised Water Reactor (PWR). The aim of the examination was to help provide an explanation for the significant variations in fatigue crack growth behaviour observed between the various specimens. Characteristic differences were observed in the appearance of the fracture surface between specimens that had shown environmentally enhanced crack growth and those that had not. Second phase sulphide inclusions were observed to have a major influence on the onset of environmentally assisted cracking. A localised influence of the test environment on the fracture surface morphology could frequently be detected even when macroscopic crack propagation rates were not enhanced. The highest crack growth rates were measured in environments which were contaminated with sulphur-bearing anions or oxidising agents.

KEY WORDS

Corrosion; fatigue; stress corrosion; cracking; fractography; fractographic; inclusions; pressure vesel steels: PWR

INTRODUCTION

Corrosion fatigue crack growth of reactor pressure vessel (RPV) steels in water reactor environments has been studied extensively in recent years, because of the importance of demonstrating that any defects which may be present in the pressure vessel cannot grow in service to reach a critical size which may result in vessel failure. The accepted procedure for assessing fatigue crack growth in this system is by use of the reference fatigue crack growth curves published in Section XI Appendix A of the ASME Boiler and Pressure Vessel Code (ASME 1983). This code includes crack growth curves for both buried defects and those which might become exposed to the reactor coolant environment, although the latter occurrence is normally prevented by an austenitic stainless steel cladding layer on the

inner vessel surface. The reference 'wet' crack growth curves are based on corrosion fatigue data obtained in simulated water reactor coolants in the 1970s (Bamford, 1980). Subsequently, a large variability in measured crack growth rates has been reported by different laboratories testing under conditions intended to simulate the primary coolant of a PWR (Bamford, 1988; Scott and Truswell, 1983; Tice, 1985). The aim of the work described in this paper was to compare the fracture surfaces of specimens exhibiting high and low crack growth rates, so as to provide an insight into the reasons for the observed variability in cracking susceptibility.

CORROSION FATIGUE TEST RESULTS

Six of the specimens were tested at two UKAEA laboratories (Harwell and Springfields), one specimen at Rolls Royce and Associates, Derby (RRA) and one at Westinghouse R&D Center. All the specimens had been tested at a cyclic loading frequency of 0.0167 Hz (with minor variations in one case) and at a loading ratio, R of 0.7. The test environments were 290°C solutions intended to simulate PWR primary coolant, although not all the simulated coolants were identical as shown in Table 1. The specimens had been manufactured from five different casts of steel with a sulphur content between 0.006 % and 0.019 % (Table 1). The detailed test results have been reported elsewhere (Atkinson and Forrest, 1985; Bamford,1988; Scott and Truswell, 1983; Tice, 1985; Tice et al, 1986) and fall into one of three categories, as summarised in Fig. 1. Several of the specimens showed negligible enhancement of the crack growth rate by the environment (e.g. D1, Fig 1) whereas others showed substantial environmental enhancement, either from the start of the test (e.g. D2) or after a period of unenhanced crack growth (e.g. C1). A characteristic of this environmentally enhanced cracking was a period when crack growth was relatively independent of the applied ΔK, indicated by a plateau region on the crack growth rate curve.

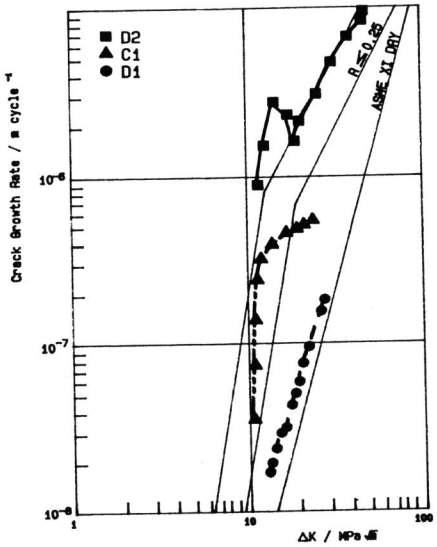

Fig. 1. Typical corrosion fatigue data for RPV steels in high temperature water.

SPECIMEN PREPARATION AND EXAMINATION

The oxide formed on all but one of the specimens during the tests was a uniform matt black colour. The layer on specimen D2 was visibly different, showing black, grey and reddish brown bands across the surface. Samples of the oxide from several of the specimens have been analysed by X-ray diffractometry (Congleton 1982). The black oxide on most of the specimens was found to be pure magnetite which is the thermodynamically stable form in deoxygenated water at around 300 C. In contrast the oxide on specimen D2 was found to contain a mixture of haematite and magnetite. The maximum

Table 1: Details of specimens tested and test conditions

Specimen	Sulphur (nominal) %	Lab.	Size mm	Orientn	Boric Acid ppm	LiOH ppm	Oxygen ppm	Hydrogen cc/kg
A1	0.006	H	25	LS	-	3	<10	40
A2	0.006	S	25	LS	10000	3	<10	-
A3	0.006	W	50	LS	-	7	<100	?
B1	0.009	S	25	LS	10000	3	<10	-
C1	0.011	RRA	50	TL	1000-10000	1	<5	10-60
D1	0.012	H	50	LS	-	3	<10	-
E1	0.019	H	50	LT	10000-13000	3	<10	40
E2	0.019	S	25	LS	10000	1	<10	-

KEY: H Harwell; S Springfields; RRA Rolls Royce & Assoc; W Westinghouse

proportion of haematite was around 35% near the crack mouth, falling along the length of the crack to below 5% near the crack tip. Fractographic examination of all the specimens was carried out in a Hitachi S450 Scanning Electron Microscope (SEM). Since the oxide layer obscured the metal surface under the SEM, the oxide was stripped from most of the samples prior to examination by using an electrolytic cleaning method in cyanide solution.

RESULTS OF FRACTOGRAPHIC EXAMINATION

Cast A, A533B plate with 0.006% sulphur

Two specimens of this steel were tested, A1 at Harwell in high flow lithiated water with added hydrogen and A2 at Springfields in low flow lithiated/borated water without hydrogen. Neither test produced significant environmental enhancement of the crack growth rate, so that rates were similar to the curve for D1 in Fig. 1. Both fracture surfaces were transgranular and uneven with microbranching (small lateral cracks leading away from the crack plane), Plate 1, and patches of ill-defined striations. At higher ΔK the quantity of microbranching, the surface roughness and the number of striations increased, the effect being greater for the Springfields specimen, A2. One isolated instance of a different fracture morphology was observed on the latter specimen, a small region of fan-shaped cracking centred on an inclusion site, Plate 2. The fracture surface within this region was more planar than the surrounding area and the tear ridges fanned out from the inclusion site.

Cast C, A533B plate with 0.011% sulphur

The one specimen from this heat, C1, had been tested at RRA in low flow borated and lithiated water with a hydrogen overpressure. The test environment was inadvertently contaminated with 2 ppm of sulphate, which was present as an impurity in the boric acid. In the early stages of the test, during which crack growth was not enhanced, the applied ΔK was stepped

in increments of 2 MPa$\sqrt{m}$. Following one of these steps, to aΔK of 22 MPa$\sqrt{m}$, there was a rapid increase in the crack growth rate (Fig. 1) to produce a period when the propagation rate was relatively independent of ΔK ("plateau" growth). At low ΔK the fracture surface was similar to that for cast A, but with rather less microbranching. The load steps were visible on the fracture surface as microscopic beachmarks but they had no affect on the mode of fracture. The sudden upturn in the fatigue crack growth rate was accompanied by a corresponding change in the fracture morphology and a decrease in the extent of microbranching. The fracture surface took on a far more fan-like appearance with associated regular striations. The change in the fracture surface took place over only 1 mm of crack growth. Only local perturbations were observed around the sulphide inclusions which were aligned parallel to the direction of crack growth and there were no observations of cracking originating from inclusion sites. The striation spacing was constant at approximately 2 μm over the full range ofΔK studied. Initially the striations appeared only in isolated regions of the surface and their spacings were much greater than the amount of crack growth per cycle. However, once the crack growth accelerated the striations became more numerous and their spacing was approximately equal to the crack extension per cycle .

Cast D, A533B plate with 0.012% sulphur

Two specimens of this material were examined. The first specimen of the two examined, D1, which had been tested at Harwell in high flowrate lithiated water without a hydrogen overpressure, produced non-enhanced crack growth rates (Fig. 1). Although the fracture surfaces were broadly similar to other specimens showing non-enhanced cracking, the extent of secondary cracking or microbranching was greater. In some instances the lateral cracking was influenced by inclusions and then the microbranches appeared larger and wider. The inclusion sites affected the local fracture morphology, often causing cracking off the main crack plane, with the area of cracking affected by an inclusion being roughly equal to its size, but the mode of fracture within the affected areas was similar to that on the rest of the fracture surface. Irregular striations were observed on the surface but only became very prominent towards the end of the test, Plate 3. There was one very small area of fan-shaped cracking observed on a secondary crack surface that had been formed under an inclusion.

The second specimen, D2, tested at Westinghouse in low flow lithiated water, produced the greatest environmental enhancement of crack growth rate amongst the specimens examined, with crack growth rates from the start of the test being about two orders of magnitude above those in air, Fig. 1. Although the fracture was transgranular as for specimens A1 and A2, the fracture surface was far more planar and exhibited noticeably less microbranching, with the tear ridges aligned in the direction of crack growth, Plate 4. The general morphology of the surface at this point was comparable to the features on specimen C1. Where the crack had intersected an inclusion there was only a limited perturbation on the fracture surface. There were no observations of fans radiating from inclusion sites, although the overall fracture surface on this specimen bore a strong resemblance to that in the fan-shaped region of specimen A2. Isolated fatigue striations were first observed 5 mm into the water fracture at a ΔK of 15 MPa$\sqrt{m}$, becoming more numerous at higher ΔK, Plate 5. These striations were much more regular and planar than those observed on specimens showing no environmental enhancement (compare Plates 1 and 5) and had a regular spacing of 2 -3μm over the whole fracture surface.

Cast E, A533B plate with 0.019% sulphur

The first of two specimens examined. E1, tested at Harwell in high flow borated and lithiated water with a hydrogen overpressure, produced non-enhanced crack growth. The fracture morphology was generally similar to that from the other tests in high flow water on casts A and D: transgranular cracking with microbranching normal to the direction of crack growth. A notable feature of this sample was the occurrence of a few areas of fan-shaped cracking, centred on inclusion sites, Plate 6, with tear ridges radiating from the centre. Each fan affected an area at least ten times greater than that of the initiating inclusion site. The fracture surface within the fan was more planar than the surrounding fracture and had no microbranching. The surface was marked by well defined regular striations normal to the tear ridges.

Specimen E2, tested at Springfields in low flow borated and lithiated water with no hydrogen overpressure, also showed little overall enhancement of cracking. The first part of the fracture surface was similar to the non-enhanced areas seen on previous specimens. However on the latter part of the fracture surface there were light grey fans up to a couple of millimetres across which were visible to the naked eye (Plate 7). The fans can be clearly seen to be located near a group of inclusion sites. The first of the fans was formed at a ΔK of about 20 MPa$\sqrt{m}$. Nearer the crack tip the fan-shaped cracking covered over half the surface area. The crack growth rate curve, Fig. 2, showed small transient increases in the rate at a ΔK value corresponding to the crack length at which the fans were formed. The fans were bounded by bands of growth typical of non-enhanced cracking. In the non-enhanced regions there appeared to be both more micro-branching and irregular striations than was normally found for non-enhanced cracking at similarΔK, producing a rougher surface than usual. Striation spacings were a constant 1 - 2μm across the specimen surface, irrespective of ΔK or the crack growth rate.

Cast B, A508-III Forging HAZ with 0.009% sulphur

This specimen, B1, had been machined from an A508-III to A508-III weldment, with the notch direction parallel to the fusion line within the heat affected zone. It was tested at Springfields in low flowrate borated and lithiated water without a hydrogen overpressure. The test history for this specimen differed from the rest because several hold periods at the maximum value of the cyclic load had been imposed to assess the possibility of any crack extension occuring under static loading, although no such crack extension had been detected. The test was started at a cyclic frequency of 0.0167 Hz and the crack growth rate was non-enhanced. There was then a period of cycling at 0.5 Hz to extend the crack length, thus increasing ΔK without increasing the loading, after which the frequency was restored to 0.0167 Hz. Enhanced crack growth occurred thereafter until a further hold was imposed at maximum load, which arrested crack growth. Resumed cycling at 0.0167 Hz produced a crack growth rate below the ASME XI air line.

The crack growth behaviour, summarised in Fig. 3, was reflected on the fracture surface. During the first part of the test, ie. before the cyclic frequency was increased to 0.5 Hz, the observed fracture morphology was typical of that already seen for non-enhanced cracking, whereas during the period of 0.5 Hz cycling typical non-enhanced features were found plus some areas resembling fan-like cracking. When the cyclic frequency was returned to 0.0167 Hz there was an immediate increase in the crack growth rate and a corresponding increase in the amount of fan-like cracking, Plate 8, until it covered a large D-shaped region in the centre of the specimen. On this part of the surface the fan-like cracking was not reliant on

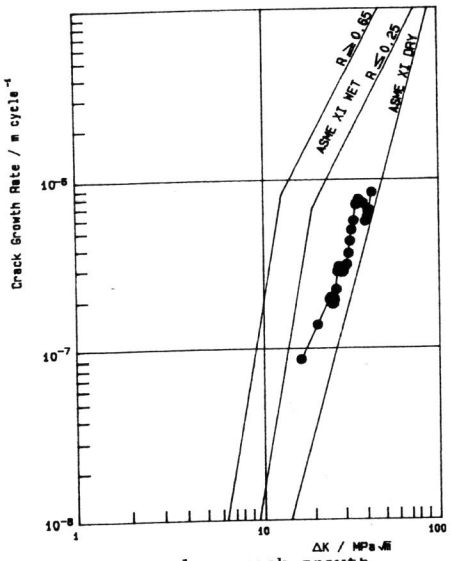

Fig. 2. Irregular crack growth curve for specimen E2.

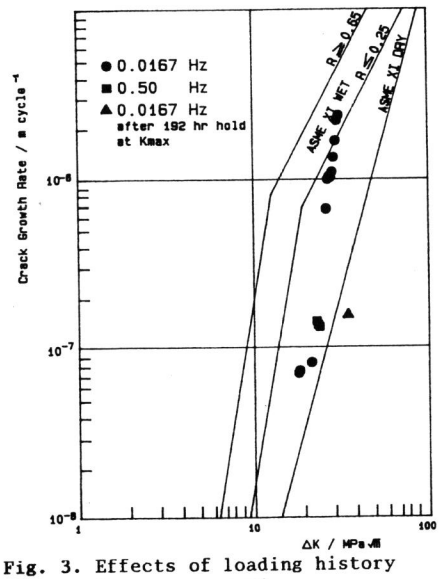

Fig. 3. Effects of loading history for specimen B1.

inclusion sites for initiation, but the inclusions did appear to affect the crack path. Further, the tear ridges and the fan-like cracking appeared to be randomly orientated as far as was possible given the constraints of the overall direction of crack growth. After the final hold at maximum load there was a small band on the fracture surface corresponding to the low growth rate measured during the final phase of the test. This region bore a strong resemblance to other regions of non-enhanced growth, i.e. a rough uneven surface with extensive microbranching and ill-defined striations.

DISCUSSION

Fracture surfaces for enhanced and non-enhanced cracking

Two distinctive types of fracture surface were observed during the fractographic examination, depending on the crack growth rate. The two surfaces can be illustrated by comparing Plates 1 and 3 with Plates 4 and 5. Plates 1 and 3 show fracture surfaces typical of non-enhanced crack growth which are characterised by a rough surface appearance, extensive microbranching and, particularly at higher values of ΔK, irregular indistinct striations. In contrast, Plates 4 and 5 illustrate fracture surfaces for a specimen producing rapid environmentally assisted crack growth. The fracture was more planar, there was only a limited amount of microbranching and the surface was marked by tear ridges orientated approximately parallel to the direction of crack growth. Where striations were observed they were sharp, well formed and aligned across the crack normal to the tear ridges.

On some of the specimens examined, both types of fracture surface were present. On the RRA specimen, a transition from one form of fracture to the other was accompanied by a rapid increase in crack growth rate whereas for

other specimens the overall crack propagation rate was not enhanced, but localised patches of enhanced growth were seen on the fracture surface, usually radiating from an inclusion site, e.g. Plates 2 and 6. Similar fractographic features have been reported by other investigators (e.g. Klemetti et al, 1984; Torronen et al, 1982; Atkinson and Bulloch, 1986). Some of these investigators have cited the apparently brittle appearance of the fracture surface on specimens showing enhanced rates of cracking as evidence for a hydrogen embrittlement mechanism of crack propagation. However, the typical features may alternatively be due to repeated dissolution at the crack tip during the straining part of the cycle. The regular striation spacing across the fracture surface may reflect the localised deformation needed at the crack tip to rupture the oxide and expose bare metal to the environment, so that crack extension is related to the duration of the straining part of the cycle and the corrosion rate of bare metal. The initial striation spacing was greater than the macroscopic crack growth per cycle suggesting that the crack extension in the early stages of a test was the average of discrete individual bursts of crack growth, whereas once full environmental enhancement was achieved the plateau crack growth rate per cycle equalled the striation spacing.

Material and environmental factors influencing crack growth

Irrespective of the actual mechanism of environmental crack advance, there is overwhelming evidence that the concentration of sulphur-containing species within the crevice environment close to the crack tip determines the extent of environmental cracking (Ford and Combrade, 1986). This local environment is normally produced by dissolution of sulphide inclusions from the steel and thus high sulphur content steels are more susceptible to environmental cracking than low sulphur steels. However the size, distribution and morphology of inclusions is also believed to be important. The presence of sulphur-bearing anions in the bulk environment provides an alternative means of retaining crack tip sulphur species, probably by reducing their rate of diffusion from the crevice, whereas high water flow rates provide a means of removal of sulphur from the crack. Oxygen or other oxidising species increase cracking susceptibility by increasing the specimen potential. One effect of an increased potential is to provide an electrochemical means of concentrating sulphur species at the crack tip. Although the majority of specimens examined showed no enhancement of the overall growth rate, a number of trends were observed from fractographic examination which were consistent with expectations based on the observed effects of material and environmental variables on crack growth rates.

Effect of sulphur: For the three steels (A,D and E) tested in one rig at high flowrate, no localised cracking was observed for the lowest sulphur content cast (A1, 0.006% S), a single isolated fan-shaped region centred on an inclusion site was found for D1 (0.012% S) and several fans for E1 (0.019% S). Similarly at low flowrate, substantially more fan shaped cracking was detected for E2 compared to A2.

Effect of flowrate: Neither of the steels A nor E which were each examined at high and low flowrate showed overall enhancement of the crack growth rate, but a significant difference was detected fractographically. Thus for each cast the test at high flow produced less localised cracking than the test in the low flow rig. For cast A there were no fans found on the surface of A1 but there was a fan on A2. For cast E there were several fans on the surface of E1 while extensive localised cracking was observed on E2.

Effect of oxisising species and sulphate contamination: Neither of these variables has been examined intentionally within this programme. However,

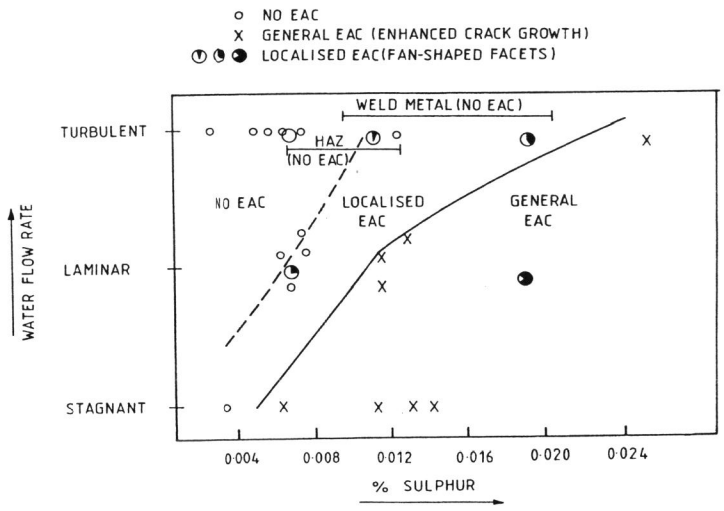

Fig. 4. Influence of steel sulphur content and water flow rate on environmentally assisted cracking (EAC)

the one test amongst the present specimens in which sulphate was known to have been present at around the 2 ppm level (specimen C1) did show sigificantly faster crack growth rates than would have been predicted from the other tests reported here. The much greater environmental enhancement for specimen D2 was probably due to an increase in the specimen potential due to the presence of an oxidant in the test environment. Evidence for the presence of an oxidising agent during at least part of the test is provided by X-ray diffractometry measurements (Congleton, 1982).

Fig. 4, due to Tice et al (1986), illustrates schematically the influence of steel sulphur content and water flowrate on environmentally assisted cracking susceptibility, based on the observation of enhanced crack propagation rates in 0.0167 Hz corrosion fatigue tests. Superimposed on the figure are data points for the specimens examined here which had been tested in good quality water. The extent of the shading of the data points indicates the degree of influence of the test environment, based on the extent of fan-shaped features indicating localised environmental cracking. (None of the specimens showed an overall enhancement of crack growth.) It is obvious from this presentation that localised environmental cracking occurs over a wider range of steel sulphur contents and water flowrate than general enhancement of crack growth, but the same parameters influence cracking susceptibility. Contamination of the test environment with sulphur anions or oxidants increases further the extent of environmental enhancement.

CONCLUSIONS

1. There is a distinct difference in the fracture surface morphology of specimens in which crack growth occurred essentially by fatigue and those in

which an environmentally influenced process such as corrosion fatigue was operative. The former is characterised by an uneven fracture surface with considerable microbranching and irregular striations, whereas environmentally assisted cracking is characterised by a planar fracture surface, a lack of microbranching and, when they occur, regular striations.

2. Most of these tests which were performed in high purity environments containing very low levels of dissolved oxygen did not show acceleration of the macroscopic crack growth rate. Nevertheless, local differences in fracture morphology were observed, indicative of localised environmental cracking.

3. The extent of localised cracking was dependent on the sulphur content of the steel, water flowrate and any sulphate contamination of the environment. These effects can be rationalised as due to the effect of these factors on the level of sulphur-containing anions at the crack tip which is the determining parameter for the onset and propagation of environmental cracking.

REFERENCES

ASME (1983). American Society of Mechanical Engineers, Boiler and Pressure Vessel Code, Section XI, Appendix A, "Analysis of Flaw Indications".

Atkinson J D, Bulloch J H and Forrest (1986). "A fractographic study of fatigue cracks produced in A533B PV steels." Proc IAEA Specialists' Meeting on Subcritical Crack Growth, Sendai, Japan, May 1985: NUREG/CP-0067, Vol 2, 269-290.

Atkinson J D and Forrest J E (1985). "Factors influencing the rate of growth of fatigue cracks in RPV steels." Corr Sci 25, 607-631.

Bamford, W H (1980). "Technical basis for revised crack growth rate curves for pressure boundary steels in LWR environment." J Pressure Vessel Tech 102, 433-442.

Bamford W H (1988). "A summary of EAC crack growyh studies performed by Westinghouse Electric Corporation under funding from the HSST programme." NUREG/CR-5020, 111-125

Congleton J (1982). Cited by Tomkins B in UKAEA Report ND-R-848(S)

Ford F P and Combrade P (1986). "Electochemical reaction rates on bare surfaces and their use in a crack prediction model for the low alloy steel/water system." Proc IAEA Specialists' Meeting on Subcritical Crack Growth, Sendai, Japan, May 1985: NUREG/CP-0067, Vol 2, 231-268.

Klemetti K, Hanninen H, Torronen K, Kemppainen M and Pessa M (1984). "On the role of inclusions in environment sensitive cracking of RPV steels." Proc Int. Symp. on Environmental Degradation of Materials in Nuclear Power Systems - Water Reactors, Myrtle Beach, Aug 22-25 1983, pp 368-383 (NACE)

Scott P M and Truswell A E (1983). "Corrosion fatigue crack growth in RPV steels in PWR primary water." ASME J Pressure Vessel Tech 105, 245-254.

Tice D R (1985). "A review of the UK collaborative programme to test the effects of mechanical and environmental variables on EAC growth of PWR PV steels." Corr Sci 25, 705-743.

Tice D R, Atkinson J D and Scott P M (1986). "A review of the UK research programme on corrosion fatigue crack propagation in PV steels exposed to PWR environments." Proc IAEA Specialists' Meeting on Subcritical Crack Growth, Sendai, Japan, May 1985: NUREG/CP-0067, Vol 1, 251-281.

Torronen K, Hanninen H and Cullen W H (1982). "Mechanisms of environment assisted cyclic crack growth of nuclear reactor pressure vessel and piping steels." Proc IAEA Specialists' Meeting on Subcritical Crack Growth, Freiburg, W Germany, May 1981: NUREG/CP-0044, Vol 2, 27-66.

AFR3-X

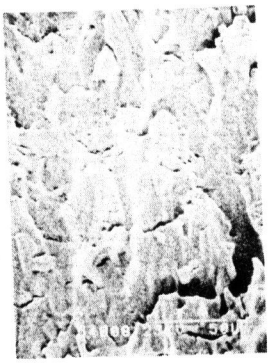

Plate 1 : A1 x 500, microbranching and irregular striations at low ΔK on a specimen showing no EAC.

Plate 2 : A2 x 400, localised fan-like cracking around inclusion site.

Plate 3 : D1 x 800, irregular striations and microbranching at higher ΔK for a specimen showing no EAC.

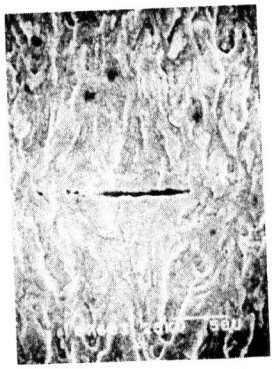

Plate 4 : D2 x 400, planar cracking at low ΔK on a specimen showing EAC.

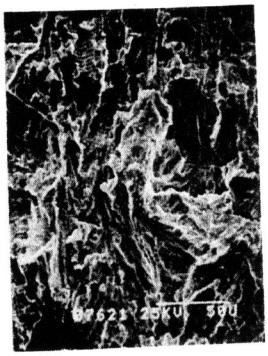

Plate 5 : D2 x 200, regular striations at higher ΔK on specimen showing EAC.

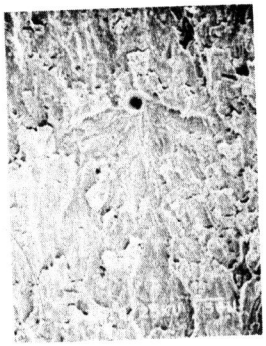

Plate 6 : E1 x 200, localised EAC around an inclusion site.

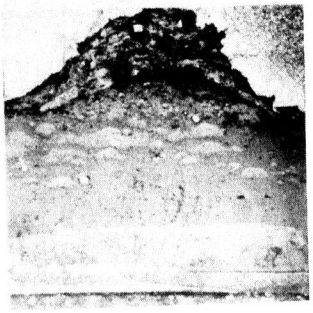

Plate 7 : B1 x 5, large areas of localised cracking in a HAZ specimen showing EAC (optical photograph).

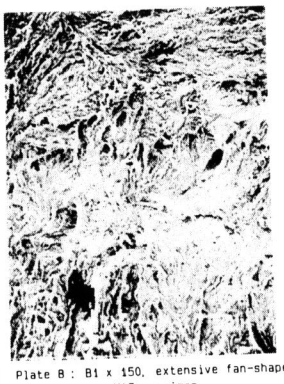

Plate 8 : B1 x 150, extensive fan-shaped cracking in a HAZ specimen.